

Robust and flexible response of *Ostreococcus tauri* circadian clock to light/dark cycles of varying photoperiod

Quentin Thommen¹, Benjamin Pfeuty¹, Florence Corellou²,
François-Yves Bouget² and Marc Lefranc^{1,3}

¹ Laboratoire de Physique des Lasers, Atomes, et Molécules,
Université Lille 1, CNRS, UMR8523,
UFR de Physique, F-59655 Villeneuve d'Ascq, France

² Laboratoire d'Océanographie Microbienne,
Université Pierre et Marie Curie, CNRS, UMR 7621,
Observatoire Océanologique de Banyuls, avenue du Fontaulé,
F-66650 Banyuls sur Mer, France

³ Corresponding author. E-mail: marc.lefranc@univ-lille1.fr

February 19, 2022

Abstract

The green microscopic alga *Ostreococcus tauri* has recently emerged as a promising model for understanding how circadian clocks, which drive the daily biological rhythms of many organisms, synchronize to the day/night cycle in changing weather and seasons. Here, we analyze translational reporter time series data of its central clock genes *CCA1* and *TOC1* for a wide range of daylight durations (photoperiods). The variation of temporal profiles with day duration is complex, with the two actors tracking different moments of the day. Nevertheless, all profiles are accurately reproduced by a simple two-gene transcriptional loop model whose parameters are affected by light only through the photoperiod value. We show that this non-intuitive behavior allows the circadian clock to combine flexibility and robustness to daylight fluctuations.

Keywords: circadian clocks; robustness; flexibility; *Ostreococcus tauri*; entrainment

1 Introduction

Most biological functions are controlled by complex networks of molecular interactions which routinely achieve sophisticated information processing and decision making. These networks, featuring manifold feedback and feedforward regulations, display a highly nonlinear collective dynamics [1–3]. A natural idea is that besides reproducing observations and checking the consistency of a biological hypothesis, mathematical modeling can help us to identify design principles at work in cellular machinery [4]. For example, it has been proposed that the oscillatory behavior of the NF- κ B transcription factor is key to its capability to integrate cellular signals of various origins and to channel them to the appropriate target [5, 6].

For this, it is essential to take into account the constraints under which evolution has tinkered over the years towards the molecular network studied [7]. Most importantly, a biological function not only has to generate an appropriate response to a given signal but to do so under predictably or unpredictably varying conditions, with cross-talk from other functions, while maintaining exquisite sensitivity. The combined requirements of robustness and flexibility have undoubtedly shaped the architecture of cell molecular networks. Accordingly, mathematical modeling has been harnessed to gain insight into the dynamical ingredients underlying such properties, which make circuits in living cells so different from a random dynamical system (see, e.g., [8–11]).

In this respect, circadian biology is a promising field [12–14]. Circadian clocks have a well defined function: they keep the time of the day so that the daily changes in the environment caused by Earth rotation can be anticipated [15, 16]. These biochemical oscillators, made of interacting genes and proteins which interact so as to generate oscillations with a period of approximately 24 hours, precisely synchronize with the day/night cycle so that stable and regular molecular ticks are scheduled. Delivering such signals in the fluctuating environment of a cell is a formidable challenge in itself, but this task is further complicated by the fact that different expression profiles must be generated as the day/night cycle varies across the year [17–19], with short days in winter and long days in summer, so as to track important moments of the day [20]. Fortunately, while understanding clock robustness is a difficult problem, assessing it only requires monitoring the circadian oscillator phase.

To understand the behavior of a functional circadian clock, the autonomous biochemical oscillator must be considered together with the day/night cycle driving it, as it is this very interaction that ensures precise time keeping. The forcing is generally parametric: one or several parameters of the internal oscillator are modulated by the external cycle, daylight being the principal cue. For example, a clock protein may be stabilized by light or degraded faster in the dark. For strong enough coupling, the phenomenon of entrainment is observed: the period of the oscillator locks exactly to that of the external forcing, ensuring that a 24-hour rhythm is generated, and a definite phase relationship between the two cycles is maintained [18, 21–24].

Thus, understanding circadian clock robustness requires identifying the needed ingredients both in the autonomous oscillations of the internal oscillator and in its response to the external driving cycle. The former question has received much attention, with special interest in the influence of intrinsic noise [25–27], due to the small number of molecules participating in the dynamics, and of temperature variations [8, 9, 28, 29]. In contrast, much less effort has been devoted to understanding how circadian clocks cope with fluctuations in forcing, even though daylight strongly fluctuates in natural conditions, throughout the day and from day to day. Thus, the same forcing cycle that synchronizes the clock to Earth rotation may also reset it erratically. Nevertheless, it has been recognized that daylight fluctuations affect entrainment accuracy [30] and recently, entrainment to natural L/D cycles has been studied more closely [31, 32]. In particular, it has been hypothesized that the need to adapt simultaneously to seasonal and weather changes has driven clock evolution towards complex architectures featuring several interlocked feedback loops [31].

Quite unexpectedly, a simple solution to this complex problem was suggested by the recent study of the circadian clock of *Ostreococcus tauri*. This green unicellular alga displays an extremely simple cellular organization [33, 34] and a small and compact genome, with low gene redundancy [35]. It shows circadian rhythms in cell division [36], and a genome-wide analysis in L/D cycles revealed rhythmic expression for almost all genes, with strong clustering according to biological process [37]. Two orthologs of central *Arabidopsis* clock genes *TOC1* and *CCA1* were identified in *Ostreococcus* genome by Corellou *et al.* [38]. Overexpression/antisense experiments supported the hypothesis that *TOC1* activates *CCA1*, which in turn represses *TOC1*, with biochemical evidence of *CCA1* binding directly to *TOC1* promoter.

This led Thommen *et al.* [39] to investigate whether a simple mathematical model of a *TOC1/CCA1* transcriptional negative feedback loop was consistent with microarray data recorded in 12:12 L/D cycles. The agreement between experimental data and a simple model based on four differential equations was excellent, providing additional support for the *TOC1/CCA1* loop hypothesis. Surprisingly, there was no signature of a coupling to light in experimental data [39], as best adjustment was obtained with a free-running oscillator model. This finding was confirmed later by adjusting simultaneously the microarray data and translational reporter data from a different experiment with the same simple mathematical model [40]

Thommen *et al.* [39] solved this paradox by noting that a precisely timed light coupling mechanism can have almost no effect on the oscillator. They exhibited several examples of coupling schemes such that an arbitrary parameter modulation inside a specific time window induces negligible deviation from the free-running profile. Such couplings are invisible when the clock is on time but can reset it very efficiently when it drifts, because coupling is then active at a time where the oscillator is responsive.

However, delicate tuning of coupling to light is not only required for shielding the clock from weather fluctuations but, perhaps more importantly, also to generate

varying clock signals across the year. A natural question is then whether the potentially conflicting requirements of robustness to fluctuations and of flexibility in the temporal profiles generated can be reconciled and satisfied simultaneously. Is robustness achieved at the cost of flexibility, or vice versa? For example, simply phase-shifting a fixed fluctuation-resistant limit cycle throughout the year would allow to track only one moment of the day.

In this paper, we advance this question by analyzing translational reporter data of the *Ostreococcus* clock genes *TOC1* and *CCA1* genes recorded for photoperiods varying between 2 to 22 hours. Quite remarkably, we observe a complex variation of time profiles with photoperiod. However, we also find that all time profiles can be accurately adjusted by the simple uncoupled clock model used previously [39, 40], provided we assume that the static control parameters of this model can vary with photoperiod. Based on our previous work [39], this suggests a clock that is robust to daylight fluctuations for all photoperiods.

That such a simple clock, with a clearly identified *TOC1-CCA1* one-loop central oscillator, is both robust and flexible is a fundamental and surprising result. It suggests that the coupling to light of the *TOC1-CCA1* loop is under control of a delicately architected web of yet unidentified additional feedback loops, which operate at different scales so as to tune separately the phase dynamics required for daily operation, on one hand, and the expression profile modifications required to adapt to changing conditions across the year, on the other hand.

2 Results

2.1 Construction of the experimental target profiles

Our analysis is based on time series data of translational reporters of the clock genes *TOC1* and *CCA1*, recorded for various light/dark sequences simulating the seasonal variations in day and night length (Fig. 1). They have been obtained in the same conditions as those analyzed by Troein *et al.* in their modeling study of *Ostreococcus* clock [41]. We did not use the transcriptional reporter data which are also available (Methods).

Cells were subjected to 24-hour cycles of alternating phases of light (L) and darkness (D), termed thereafter day and night. Two experiments were conducted, where day lengths for different cell cultures ranged from 2 to 12 hours (Fig. 1 A–F), and from 12 to 22 hours (Fig. 1 G–L), respectively. For each cell culture, the lighting protocol began with two cycles where photoperiod (day length) was 12 hours (0–48 hours), followed by three cycles (termed below photoperiodic cycles) with a photoperiod between 2 and 22 hours (48–120 hours), the last cycle being under constant illumination (120–144 hours). The two time series with a photoperiod of 12 hours (LD 12:12), one in each experiment, have similar profiles although the timings differ slightly. Time series corresponding to different cell cultures subjected to the same lighting sequence are very consistent, showing the high reproducibility

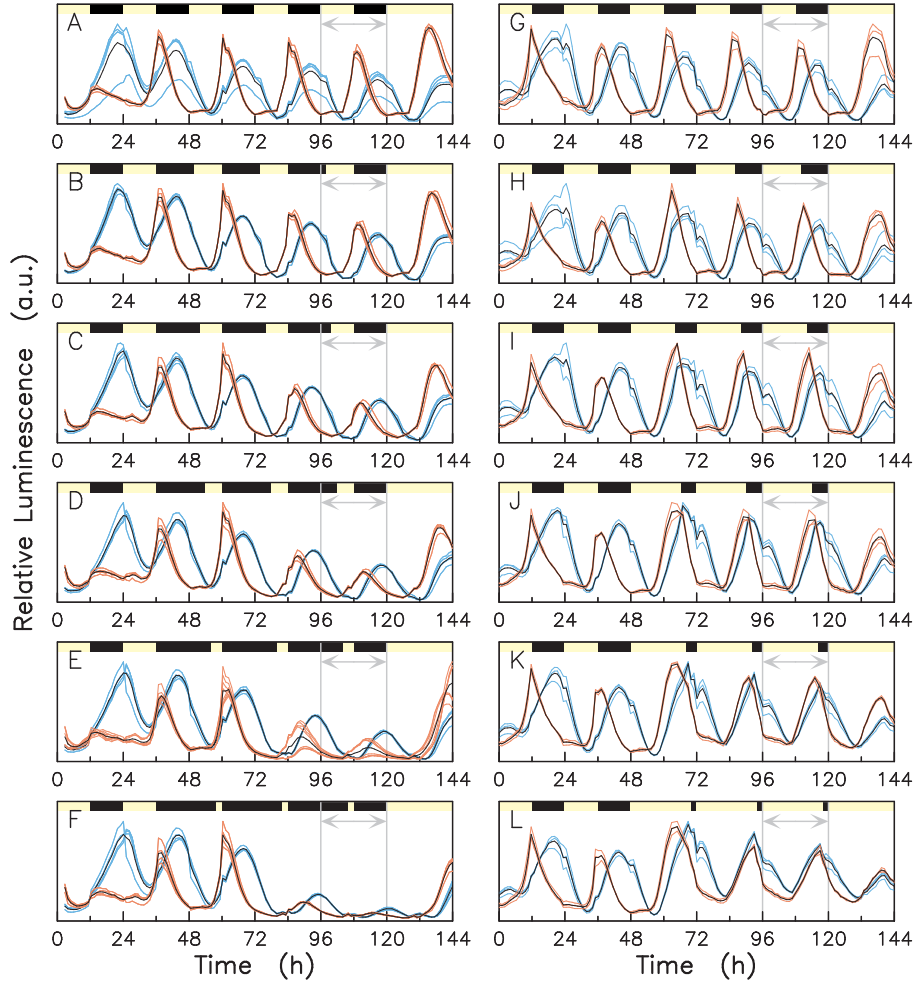


Figure 1: Photoperiodic response of core clock components. *Ostreococcus* TOC1:LUC (red) and CCA1:LUC (blue) translational reporter lines were entrained under 24-hour day/night cycles with varying day length (A: 12h; B: 10h; C: 8h; D: 6h; E: 4h; F: 2h; G: 12h; H: 14h; I: 16h; J: 18h; K: 20h; L: 22h). Yellow and black bars at the top of each panel indicate periods of light and darkness, respectively. Averages of translational reporter lines are drawn as black solid lines. The time interval between 96 and 120 hours contains data used for model adjustment.

of the data, and motivating a quantitative description of experimental data by a mathematical model based on biochemical kinetics.

Our goal is to better understand how *Ostreococcus* clock entrains to different cycles across the year. How do the entrained temporal profiles of the two clock genes *TOC1* and *CCA1*, and in particular their peak timings, vary with photoperiod? Is the apparent invisibility of coupling previously evidenced in LD 12:12 experiments [39, 40] observed for all photoperiods? Therefore, we focus here on reproducing data from the third photoperiodic cycle (between 96 and 120 h), assuming that *Ostreococcus* clock has by then acclimated to the photoperiod change

applied at time 48 h, and displays its nominal response to the entrainment cycle. This 24-hour interval of time is indicated with a two-head gray arrow in Fig. 1.

The time series shown in Fig. 1 give us the total luminescence emitted by a cell population. As such, they may reflect the average single-cell clock dynamics as well as variations in the total number of cells or their spatial distribution. For example, cell cultures are expected to grow faster in long days since the number of cell division events per day was shown to increase with day length [42]. In contrast to this, we expect that the shape of the temporal expression profiles, and in particular their peak timings, essentially provides information related to the clock dynamics. To avoid capturing amplitude variations possibly biased by population dynamics, we normalize the data for the different photoperiods so that they have the same maximum expression level.

In order to keep the mathematical model as simple as possible and avoid over-fitting the data, we moreover neglect the fact that luminescence is generated by reporter genes inserted into the genome in addition to the wild ones (possibly inducing overexpression effects). We use the translational reporter time series as indicators of native protein concentration, an approximation which has been checked in our previous works [39, 40] and which is acceptable when the photon emission time is much larger than the protein degradation time. In fact, a fully detailed model would have the simple model described below as limiting case, and would only be needed to improve adjustment. Finally, we remove the floor level bias evidenced by Morant et al. [40] to obtain the target profiles.

2.2 Circadian phases of *TOC1* and *CCA1* display a complex variation with photoperiod

Before carrying out any adjustment, the analysis of the target profiles reveals a complex orchestration of *CCA1* and *TOC1* expression by *Ostreococcus* clock, despite its apparent simplicity. This is illustrated by Fig. 2, which displays the time positions of *TOC1* and *CCA1* expression peaks as a function of Zeitgeber Time (ZT), measured from last dawn. It appears clearly that the *TOC1*–*CCA1* oscillator does not respond to varying photoperiod by simply globally shifting its phase but relies on a mechanism that controls differentially the peak timings of *CCA1* and *TOC1*. *TOC1* peak tends to track dusk except for very short days where its timing becomes roughly fixed relative to dawn. For long days, *CCA1* peak tracks dawn, occurring around ZT21, while for short days it combines information about both dawn and dusk, occurring approximately one hour after the middle of the night.

The time delay between *TOC1* and *CCA1* expression peaks, as well as their times of occurrence in the lighting cycle, are therefore critical clock features. One objective of this work is to check whether the variations of *TOC1* and *CCA1* temporal profiles with photoperiod, including interpeak delay and peak widths, can be reproduced by a mathematical model. Interestingly, it is for the pivotal case of LD 12:12 that the *TOC1*–*CCA1* delay is larger and the expression peaks narrower. As

the interpeak delay decreases, above or below a photoperiod of 12 hours, expression peaks tend to broaden.

For each photoperiod, the relative position of the two expression peaks remains compatible with the hypothesis of a two-gene loop where *TOC1* activates *CCA1* and *CCA1* represses *TOC1*, except for a photoperiod of 22 hours, where the two peaks coincide. Our assumption that luminescence signals reflect true protein concentrations reaches then its limits. Recall that luminescence data of *CCA1-LUC* and *TOC1-LUC* come from different cell lines. Insertion of *CCA1-LUC* (resp. *TOC1-LUC*) induces an overexpression of *CCA1* (resp. *TOC1*), which can be shown to shorten (resp. lengthen) the free-running period (FRP). These opposite FRP variations result in slight antagonist phase shifts of expression profiles, leading to overlap of the expression peaks. This problem could be worked around simply by using more detailed models of the two transgenic clocks (including the *CCA1-LUC* and *TOC1-LUC* genes), however we will see later that this would only be needed for extreme photoperiods, encouraging us to preserve the simplicity of our model.

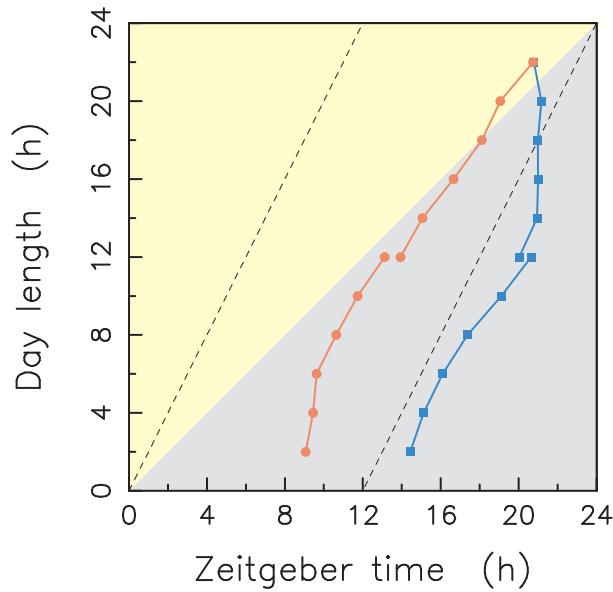


Figure 2: Complex response of *Ostreococcus* clock to photoperiod changes. Timing (ZT) of the concentration peaks of *TOC1:LUC* (red) and *CCA1:LUC* (blue) are shown as a function of day length. The yellow and gray backgrounds indicate intervals of light and darkness, respectively. Dashed lines correspond to middle of the day and middle of the night.

2.3 Mathematical model

The minimal model of the *TOC1-CCA1* transcriptional feedback loop consists of the following four ordinary differential equations:

$$\dot{M}_T = \mu_T + \frac{\lambda_T}{1 + (P_C/P_{C0})^{n_C}} - \delta_{M_T} \frac{K_{M_T} M_T}{K_{M_T} + M_T} \quad (1a)$$

$$\dot{P}_T = \beta_T M_T - \delta_{P_T} \frac{K_{P_T} P_T}{K_{P_T} + P_T} \quad (1b)$$

$$\dot{M}_C = \mu_C + \frac{\lambda_C (P_T/P_{T0})^{n_T}}{1 + (P_T/P_{T0})^{n_T}} - \delta_{M_C} \frac{K_{M_C} M_C}{K_{M_C} + M_C} \quad (1c)$$

$$\dot{P}_C = \beta_C M_C - \delta_{P_C} \frac{K_{P_C} P_C}{K_{P_C} + P_C} \quad (1d)$$

Eqs. (1) describe the time evolution of mRNA concentrations M_C and M_T and protein concentrations P_C and P_T for the *CCA1* and *TOC1* genes, respectively, as they result from mRNA synthesis regulated by the other protein, translation and enzymatic degradation. *TOC1* transcription rate varies between μ_T at infinite *CCA1* concentration and $\mu_T + \lambda_T$ at zero *CCA1* concentration according to the usual gene regulation function with threshold P_{C0} and cooperativity n_C . Similarly, *CCA1* transcription rate is μ_C (resp., $\mu_C + \lambda_C$) at zero (resp., infinite) *TOC1* concentration, with threshold P_{T0} and cooperativity n_T . *TOC1* and *CCA1* translation rates are β_T and β_C , respectively. For each species X , the Michaelis-Menten degradation term is written so that δ_X is the low-concentration degradation rate and K_X is the saturation threshold. Their expression is mathematically equivalent to the usual formulation using the Michaelis-Menten constant K_X and the maximum degradation speed $V_{\max} = \delta_X K_X$.

We had found previously that Eqs. (1) with no parametric modulation, corresponding to a free-running oscillator, could reproduce simultaneously microarray and translational reporter data recorded under two different LD 12:12 experiments, with excellent agreement [40]. To evaluate adjustment reproducibility, we checked whether Eqs. (1) using the best-fitting parameter set obtained in [40] could reproduce the two LD 12:12 datasets used here. As Fig. 3 shows, there is an excellent agreement with the short-day experiment recording, which is the third experiment adjusted by this model with this parameter set! For the long day experiment, there is a noticeable shift in the *CCA1* peak, which is not understood. As we see below, however, this will not affect our main conclusions.

2.4 Photoperiod-dependent free-running oscillator models adjust experimental data precisely

A simple way to obtain a robust coupling for all photoperiods would be to globally phase shift the robust oscillator evidenced in previous work [39, 40] depending on photoperiod, keeping the two profiles and their separation unchanged. However, the

very fact that TOC1–CCA1 delay and peak widths vary significantly with photoperiod totally excludes such possibility. It is then quite mysterious how robustness can be achieved simultaneously for each of the different profiles observed.

In order to gain insight into how robustness combines with the flexibility observed, we tested adjustment of the expression profiles profiles by free-running TOC1–CCA1 oscillator models whose parameters are allowed to vary with photoperiod. This amounts to carrying out for each photoperiod the same analysis that we applied to a LD 12:12 dataset in our previous works [39,40]. Parameter values of model 1 are optimized to adjust this model to the experimental profiles under the constraint that the FRP is 24 hours (as discussed in [39], this technical simplification does not imply that the actual FRP is exactly 24 hours).

Fig 4-A shows clearly that an impressive agreement between experimental and numerical profiles can be obtained for all photoperiods. In particular, the timings of the TOC1 and CCA1 expression peaks are very well reproduced (Fig. 4-B). By applying the same procedure to random target profiles, we found that the probability of obtaining such a good agreement for all photoperiods by chance is exceedingly low, well below 10^{-4} (Methods). Thus, this finding strongly suggests that a strong evolutionary constraint has shaped the expression profiles of *Ostreococcus* clock. If our interpretation of the invisible coupling behavior is correct, this constraint is the necessity of maintaining robustness to daylight fluctuations all across the year.

That *Ostreococcus* clock generates time profiles which remain so close to that of a free-running oscillator while strongly varying with photoperiod is a very important result. It shows that robustness and flexibility can be simultaneously achieved in a simple clock built around a simple one-loop, two-gene, core oscillator. This flexibility appears clearly in Fig. 4-C, which shows the projections into the TOC1–CCA1 plane of the different limit cycles observed for all photoperiods.

For each photoperiod, excellent adjustment was obtained in a wide region of pa-

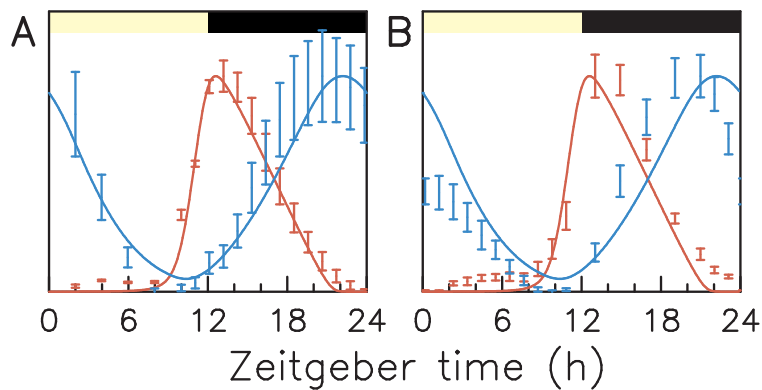


Figure 3: Comparison of data recorded in LD 12:12 with numerical solutions of model (1) using the parameter set obtained in Ref. [40]. TOC1 (resp., CCA1) profiles are drawn in red (resp., blue). (A) Short-day experiment, corresponding to signal in Fig.1-A; (B) Long-day experiment, corresponding to signal in Fig.1-G.

parameter space (see [39] for more details), a phenomenon which is often observed in systems biology models [43]. Independent adjustments for each photoperiod therefore yield wildly varying parameter values as a result. We therefore used a modified goodness of fit estimator penalizing parameter value dispersion across photoperiods, to ensure that parameter value variations across the photoperiod range were only as large as needed to reproduce the different time profiles. Fig. 5 shows the obtained parameter values vary as a function of photoperiod. For most parameters, a limited and smooth variation with photoperiod is observed, consistent with the idea of a tuning of the TOC1–CCA1 loop depending on photoperiod. The parameter values for the two LD 12:12 experiments are generally relatively consistent between themselves as well as with the parameter values obtained in [39].

It is difficult to assess the biological significance of these curves at this stage because time series are purposely adjusted up to a scaling both in concentrations and in time (to keep the FRP at 24 hours). While this guarantees that only the clock dynamics is probed, possible systematic variations in expression levels with photoperiod are not captured and should manifest themselves as systematic variations in the best fitting parameter values (Methods). It is thus plausible that less parameters do vary with photoperiod than appears in Fig. 5. However, we concentrate here on our strategy to evidence the free-running behavior of the TOC1–CCA1 oscillator at all photoperiods, leaving precise parameter estimation for a future work.

2.5 Robustness to daylight fluctuations

Here we illustrate how robustness to daylight fluctuations can be achieved with a light coupling mechanism that does not visibly affect the dynamics of the core oscillator in entrainment conditions. As an example, we will assume that the core TOC1–CCA1 oscillator is driven by the day/night cycle via a transient modulation of parameter δ_{P_T} (TOC1 degradation rate). For the sake of simplicity, this modu-

Table 1: Parameter values obtained by adjusting experimental data with a free-running model with 16 photoperiod-dependent parameters

	Ref [40]	Short day experiments							Long day experiments						
Day length	12	2	4	6	8	10	12		12	14	16	18	20	22	
RMS Error	7.85	7.3	4.5	3.7	3.5	3.8	4.5		5.3	4.6	5.9	7.4	9.0	9.7	
n_T	2	2	2	2	2	2	2		2	2	2	2	2	2	
μ_C (nM.h ⁻¹)	0.153	0.262	0.174	0.216	0.163	0.227	0.197		0.626	0.379	0.787	0.871	0.622	0.235	
λ_C (nM.h ⁻¹)	3.10	7.43	3.56	3.49	2.54	2.98	2.45		3.04	3.34	3.99	3.56	2.72	2.46	
P_{T0} (nM)	18.7	48.1	38.8	38.5	35.4	36.8	26.8		37.0	42.6	26.3	26.6	21.8	16.2	
β_C (h ⁻¹)	2.83	4.90	4.52	4.48	5.71	5.34	4.77		5.72	10.3	7.88	9.29	13.1	15.5	
n_C	2	2	2	2	2	2	2		2	2	2	2	2	2	
μ_T (nM.h ⁻¹)	0.467	2.54	2.82	2.50	2.58	2.59	2.96		2.54	2.54	3.20	3.20	3.22	2.92	
λ_T (nM.h ⁻¹)	487	108	86.0	84.5	108	84.9	86.0		101	79.8	93.9	93.2	90.2	94.1	
P_{C0} (nM)	4.51	14.9	8.06	7.90	6.52	5.57	7.24		4.89	6.78	5.11	4.87	4.90	6.00	
β_T (h ⁻¹)	0.812	0.072	0.105	0.135	0.185	0.457	0.801		0.157	0.226	0.086	0.063	0.037	0.024	
$1/\delta_{M_C}$ (h)	0.195	0.137	0.193	0.205	0.232	0.183	0.209		0.245	0.274	0.245	0.275	0.423	0.376	
$1/\delta_{P_C}$ (h)	2.36	2.91	1.86	1.68	1.68	1.83	2.08		1.16	0.654	0.444	0.370	0.286	1.79	
$1/\delta_{M_T}$ (h)	0.129	0.074	0.097	0.098	0.103	0.114	0.119		0.106	0.107	0.115	0.120	0.125	0.122	
$1/\delta_{P_T}$ (h)	0.199	0.538	0.644	0.630	0.400	0.318	0.273		0.394	0.339	0.533	0.563	0.479	0.105	
κ_{M_C} (nM)	0.407	0.303	0.250	0.250	0.268	0.274	0.273		0.345	0.303	0.407	0.463	0.559	3.364	
κ_{P_C} (nM)	75.9	2237	1386	1258	1168	1105	843		1579	2239	12054	13648	14678	10575	
κ_{M_T} (nM)	28.3	8.25	8.17	8.09	9.21	6.70	7.72		6.68	6.65	7.22	6.93	7.51	5.70	
κ_{P_T} (nM)	2.76	2.50	2.98	3.04	2.99	3.71	3.31		2.91	2.79	3.24	3.12	1.70	0.273	

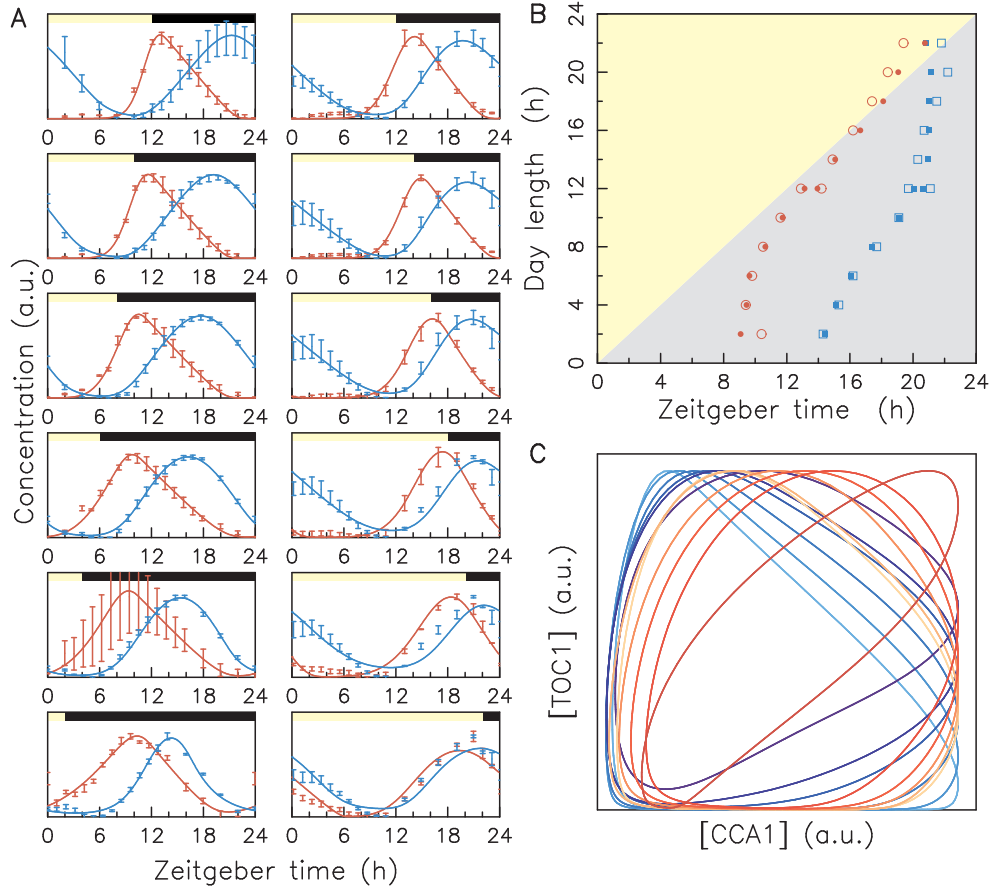


Figure 4: Adjustment of TOC1 and CCA1 profiles by a free-running oscillator model. (A) Measured data shown in Figure 1 are compared with numerical solutions of a free-running oscillator model (Eqs. (1)) where all parameters have been adjusted for each photoperiod. (B) Comparison of the ZT peak timings of TOC1 (red circles) and CCA1 (blue squares) expression, for experimental data (full symbols) and model (empty symbols). An excellent agreement is observed both for profile shapes and timings. (C) Projection of the limit cycle into the TOC1–CCA1 plane for the different photoperiods. Line color indicates photoperiod, and ranges from dark blue (2-hour day length) to dark red (22-hour day length), light blue and light red corresponding to short-day and long-day 12:12 protocols, respectively.

lation occurs in a temporal window which is fixed relative to the day/night cycle. There is no loss of generality in doing so if we only intend to understand the behavior in entrainment, not the dynamics of resetting after a large phase excursion. How such a parametric forcing ensures a stable phase relation between the clock and the day/night cycle can be understood as follows.

The action of a parametric modulation on an oscillator is described by the impulse phase response curve (iPRC) [8, 32, 44], which gives the phase shift induced by a short parameter perturbation with unit time integral as a function of the position

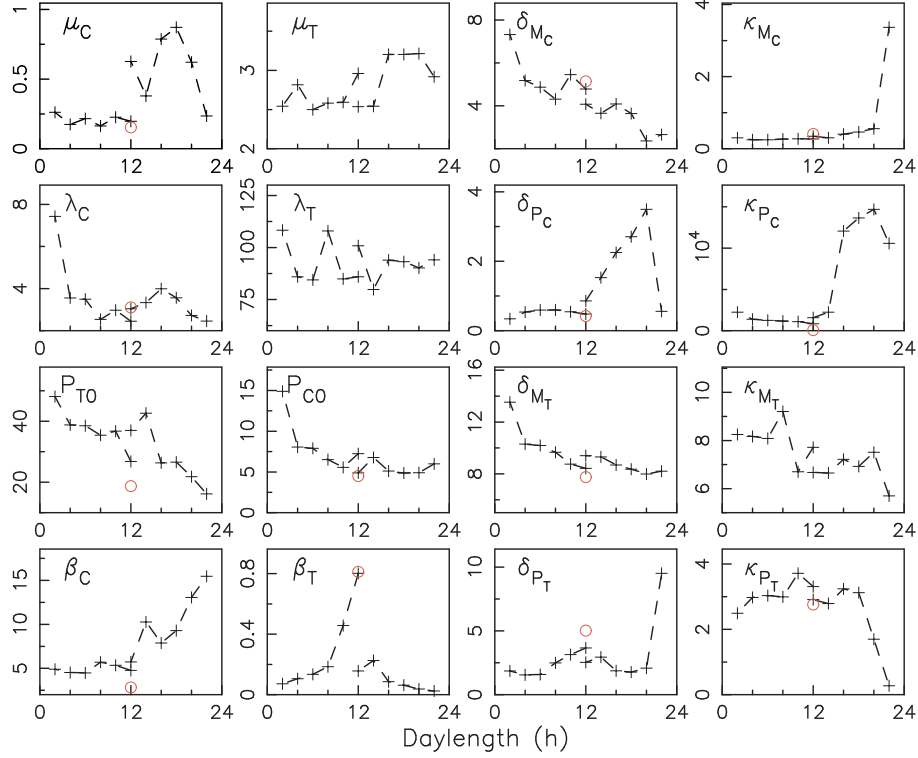


Figure 5: Values of the best-fitting parameters used in Fig. 4 as a function of photoperiod. The red circle indicates the parameter value adjusted in Ref. [40].

along the limit cycle. Fig. 6-A shows the iPRCs of TOC1 degradation modulation computed for the entrained limit cycles observed at varying photoperiods. Although the shape of these iPRC slightly varies for these distinct limit cycles, it is remarkable that the flat part of the iPRC persists. This conserved feature of the iPRC, also known as a dead zone, reflects an insensitivity of the limit cycle to TOC1 degradation modulation at the beginning of the day. This implies that the coupling profile can be designed so as to match these intervals of insensitivity, endowing the clock with robust entrainment by fluctuating forcing [44].

It is to note that, in the limit of weak coupling, the total phase shift $\delta\phi$ induced by parameter perturbation profile $\delta p(t)$ is given by $\delta\phi = \int_{t_{\text{on}}}^{t_{\text{off}}} Z(t) \delta p(t) dt$ where $Z(t)$ is the iPRC and t_{on} and t_{off} are the start and end times of the coupling window. For a FRP of approximately 24 hours, stationary operation requires $\delta\phi \approx 0$ so that the coupling window $[t_{\text{on}}, t_{\text{off}}]$ must be located around a zero of the iPRC $Z(t)$ (a stable operation also requires a negative derivate of $Z(t)$ at this zero).

For each photoperiod, we searched for coupling windows inside which TOC1 degradation can be increased without degrading model adjustment compared to the uncoupled model. This is in principle a stringer requirement than the zero phase shift condition since this also implies that the deviation from the limit cycle is minimal. Fig. 6-B shows the locations of such windows where coupling activation was

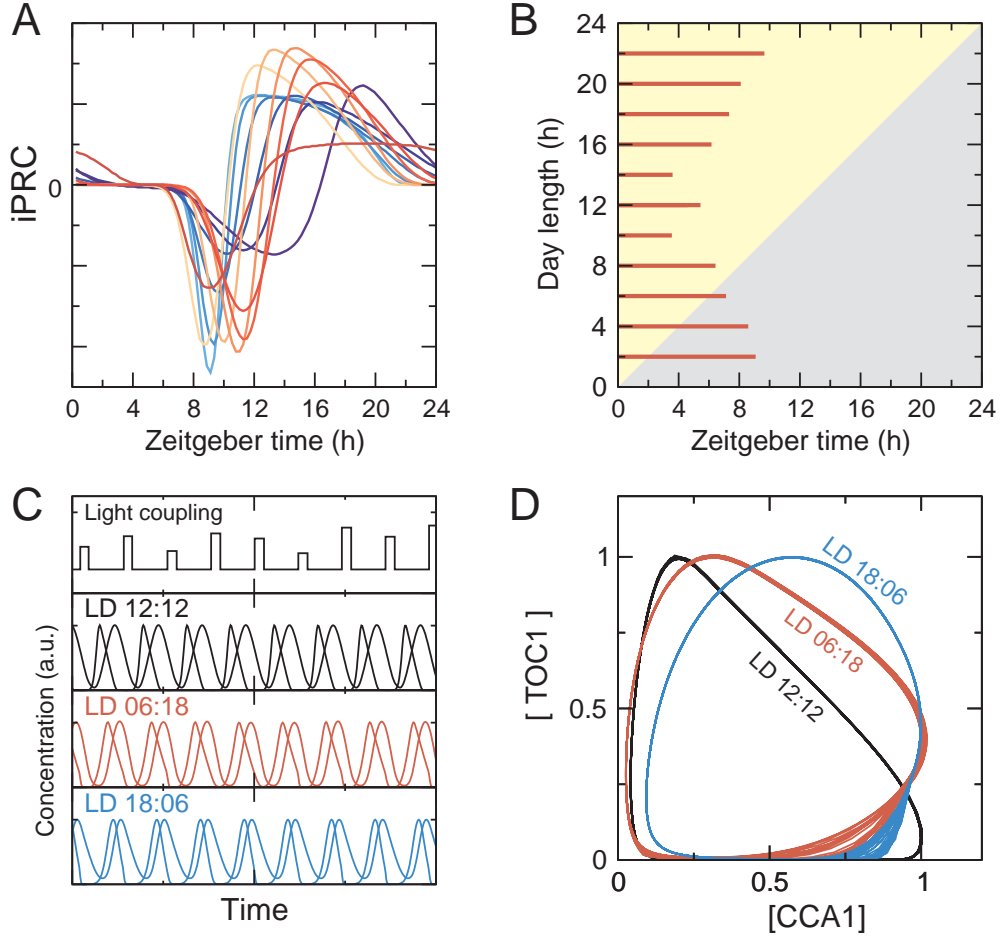


Figure 6: Robust coupling to light at all photoperiods. (A) Phase Response Curves (iPRCs) of the different photoperiod-dependent free-running oscillators in response to an impulse perturbation of TOC1 degradation rate. (B) Coupling windows in which TOC1 degradation rate is multiplied by two and beginning at ZT0 such that adjustment of model to experimental data is preserved (no deformation of the limit cycle). (C) Entrained TOC1/CCA1 oscillatory profiles are insensitive to fluctuations of TOC1 degradation rates (modulation factor uniformly distributed between 1 and 3) inside the coupling windows in Panel B. (D) Limit cycles corresponding to the profiles shown in Panel C, showing the small residual fluctuations.

fixed at ZT0 and increase of TOC1 degradation rate during the coupling window at 100 %. In fact, the timings of these windows almost did not depend on the modulation factor chosen, indicating that the same limit cycle, close to the uncoupled one, is obtained at different coupling strengths (hence light levels). Interestingly, window timings are relatively symmetrical around the LD 12:12 protocol.

As Fig. 6-C shows, this insensitivity of the adjustment with respect to modulation strength ensures that the circadian oscillator is robust to daylight fluctua-

tions. We subjected the limit cycles obtained for three different photoperiods (LD 12:12, LD 6:18 and LD 18:6) to a random sequence of modulation depths. On each day, TOC1 degradation rate was multiplied inside the coupling window shown in Fig. 6-B by a random factor uniformly distributed between 1 and 3. This describes adequately the effect of daylight variations from one day to the next, which are the most disruptive because they are resonant with the oscillator [39]. It can be seen that the circadian clock ticks very robustly in the three cases, delivering signals almost identical to those of a free-running oscillator even though there is a strong coupling operating for several hours (Fig. 6-B). Obviously, this only holds when the oscillator has the phase observed experimentally. Otherwise, the zero phase shift condition is not satisfied and the coupling rapidly resets the clock to the correct time.

Fig. 6-D displays the three limit cycles under random forcing, showing the small residual fluctuations. Interestingly, these are stronger for the two extreme photoperiods than for the LD 12:12 protocol which is impressively insensitive to fluctuations. This figure, with its clearly distinct limit cycles, illustrates nicely how robustness to daylight fluctuations and flexibility can be combined in a simple clock provided coupling to light is suitably designed.

To summarize this section, adjustment of circadian signals by a free-running oscillator model does not imply that there is no coupling, but rather that coupling is scheduled so that it does not affect the oscillator when the clock is entrained, thereby shielding it from daylight fluctuations. Importantly, it was shown in [39] that even when the free-running period is different from 24 hours, a similar mechanism is possible. Coupling then acts to rescale the oscillation period to 24 hours, but leaves no other print besides a small amplitude variation, as the waveforms can be adjusted by a free-running oscillator model.

3 Discussion and Conclusion

In this work, we have studied the response of *Ostreococcus* circadian clock to day/night cycles of various day lengths, such as those induced by seasonal changes. The analysis of the photoperiod-dependent expression profiles of the two central clock proteins TOC1 and CCA1 allowed us to unveil two remarkable features of *Ostreococcus* clock photoperiodic behavior.

First, a flexible and complex variation of expression profiles with photoperiod is observed, reminiscent of that observed in the higher plant *Arabidopsis* [20]. There is not only a complex response of the oscillator phase to varying photoperiod [41] but also the time interval between the two expression peaks and the waveform of the profiles change significantly with photoperiod. More precisely, TOC1 expression tends to follow the day-night transition, except in shorter days where it remains fixed relatively to dawn, whereas CCA1 expression is scheduled in the middle of the night, except for longer days where it tracks dawn (Fig. 2). Therefore, at least two phases rather than a single one are needed to describe entrainment of *Ostreococcus* clock to different photoperiods. More generally, it is consistent with the view that a

circadian clock must deliver different signals in different seasonal contexts because different physiological processes must be controlled at different times of the day, which is indeed the case in *Ostreococcus* [37].

Second, we found that protein expression data for all photoperiods can be adjusted with surprising accuracy by a minimal model of the TOC1–CCA1 transcriptional loop with no driving by light, provided that its kinetic parameters are allowed to vary with photoperiod to account for the flexible response observed. This remarkable finding not only confirms the central role of the TOC1–CCA1 loop in *Ostreococcus* circadian clock [39–41, 45] but also indicates that the light coupling mechanisms which synchronize the clock become invisible when the clock is entrained. As we showed, a simple explanation for this phenomenon is that activation of the light input pathway coincides with a “dead zone” of the phase response curve of the circadian oscillator [44]. Such a design ensures that the same profiles are generated at different daylight intensities, in which case random fluctuations have no effect. This finding suggests that molecular signals from this clock have been strongly shaped by the requirement of being robust to daylight fluctuations all along the year. This constraint is all the stronger in *Ostreococcus* as the light perceived by this marine organism varies not only due to sky cover but also depending on distance to surface and water turbidity.

Flexibility and robust synchronization to the day/night cycle both rely on the architecture of the light input pathways and feedback loops interacting with the TOC1–CCA1 oscillator, about which little is currently known despite recent progress [46, 47]. Together, our results suggest that there is a clear distinction of light coupling processes according to dynamical role and time scale.

On the one hand, gated coupling mechanisms, where a kinetic parameter is modulated for a few hours, are required to ensure entrainment and keep the oscillation phase stable from day to day. Gated light inputs is a feature of many circadian clocks and it has been proposed that they are critical for generating appropriate timings under different photoperiods [18]. Closely related phenomena are light adaptation or response saturation [32, 48, 49]. We have proposed that in a robust clock, the fast synchronizing inputs must be tuned so that they do not deform the entrained limit cycle, which would otherwise be exposed to daylight fluctuations [39]. Therefore, the flexible variation of expression profiles with photoperiod needed to adapt clock signals to different seasons must entirely rely on slow inputs modifying kinetic parameters of the core oscillator on a time scale of several days. Indeed the existence of such slow kinetic changes naturally explains why the variation of expression profiles with photoperiod is perfectly matched by a free-running oscillator model with photoperiod-dependent parameters. Such slow changes may be related to light accumulation processes, coincidence mechanisms or metabolism, and more generally to the presence of molecular actors constitutively expressed at photoperiod-dependent levels. In fact, this separation in fast mechanisms maintaining phase and slow mechanisms controlling expression profiles is only a necessary condition for robustness, as the synchronizing couplings and their phase response curves must also satisfy

specific constraints to ensure a reproducible phase dynamics over a wide range of operating conditions [44].

Admittedly, implementing the design principles we have unveiled in a detailed mechanistic model of *Ostreococcus* clock is not an easy task, if only because of the number of slow inputs needed to reproduce the variation of expression profiles with photoperiod. In this respect, it would be interesting to analyze the *Ostreococcus* clock model proposed by Troein *et al.* [41] in the light of our results. This model, which takes into account the detailed dynamics of the luminescent reporters, was constructed from an extensive dataset obtained in essentially the same experimental conditions as our time series. Both limit cycle profiles and transient behavior (change in photoperiod, transition into constant light) were taken into account to adjust the mathematical model. Troein *et al.* concluded that the complex behavior of the one-loop *Ostreococcus* clock could be explained by the presence of five different light inputs into CCA1–TOC1 loop, seemingly contradicting our results. It may be that these light inputs are gated by the profiles of the actors they affect. Interestingly, the profiles generated by this model are relatively smooth, except at dawn and dusk, which could indicate a weak effective coupling. Otherwise, the light accumulator present in this model is similar to a slow input, although it seems to be operating on a time scale too short to ensure robustness, and probably cannot reproduce alone the flexibility observed in expression profiles.

It is also interesting to compare our results to Ref. [20] where the flexibility of increasingly complex model of *Arabidopsis* clock was studied and compared to experimental results. It was shown that mechanistic models of this circadian require at least three feedback loops to generate timing patterns that are not limited to tracking dawn or dusk and which reproduce those observed experimentally. This finding is consistent with the theoretical prediction that flexibility requires several interlocked feedback loops [8, 9, 50]. Yet, it seems that a one-loop model with photoperiod-dependent parameters is able to reproduce very complex patterns where, for example, CCA1 can track dawn or the middle of the night depending on photoperiod. This suggests that more attention should be given to the role of slow light inputs, serving as photoperiod sensors. Such slow effects of light have been recently evidenced in mice [51]. It is probably the case that in *Ostreococcus*, these slow inputs are controlled by additional feedback loops that remain to be discovered. What complicates their identification is that they seem to be invisible in entrainment conditions by design.

Clearly, *Ostreococcus* clock has not yet revealed all its secrets. Our partial results suggest that unraveling them may unveil important design principles in circadian biology, thanks to the surprising agreements between mathematical models and experimental data that can be obtained in this model organism. Whatever molecular model of *Ostreococcus* clock eventually emerges, an important lesson from *Ostreococcus* clock response to photoperiod changes will undoubtedly be that even a simple circadian clock can combine robust and flexible mechanisms to adapt to changing weather and seasons.

4 Methods

4.1 Experimental data

The experimental data were obtained as described by Corellou *et al.* [38], in essentially the same experimental conditions as used by Troein *et al.* [41]. We did not use the transcriptional reporter data available. Indeed, Djouani-Tahri *et al.* [46] showed directly, using inhibitors of translation, that the time between luciferase synthesis and photon emission is extremely long, of the order of 8-10 hours. This is the time required to observe a significant decrease in luminescence when translation is blocked. A conclusion of our previous works [39,40] is that transcriptional activities of both *TOC1* and *CCA1* are confined to much shorter time interval. As a result, the signal of interest, namely transcriptional activity, is probably averaged out in the transcriptional reporter luminescence data, which may destabilize the adjustment procedure

4.2 Target profiles

The target profiles of protein concentration are obtained from the luminescence records of the translational reporter lines during the third cycle of photoperiod (from 96 h to 120 h in Fig 1). Luminescence time series display variations in amplitude from day to day due to fluctuations in the number of cells contributing to light emission and other unknown factors. To correct this effect approximately and obtain periodic target profiles, the time series were divided by a first order polynomial function of time interpolating between the luminescence intensities at 96 h and 120 h. The floor level was then removed from the time series to correct for the bias evidenced in [40] and periodic profiles for all photoperiods were then rescaled to have the same maximum value.

4.3 Adjustment and goodness of fit

Model (1) has 16 free continuously varying parameters besides the cooperativities n_C and n_T which are set to the integer values 2. Two solutions of Eqs. (1) that have the same waveforms up to a scale factor are considered equivalent. Although this allows us to factor out population effects, this makes it more complicated to compare parameter sets resulting from optimization, because each one is actually the representative of a four-dimensional manifold of equivalent points in parameter space. This is adequate for our purposes since our goal here is to establish the relevance of the free-running TOC1–CCA1 oscillator model for all photoperiods, not to estimate accurate parameter values. To measure the goodness of fit for a given parameter set, the two numerical protein profiles are rescaled to have the same maximum value as the experimental profiles and compared to the latter by computing the root mean square (RMS) error.

4.4 Optimization

Adjustment was carried out by using a population-based metaheuristic method (harmony search [52]) for the initial large-scale search, followed by a nonlinear optimization procedure based on a Modified Levenberg–Marquardt algorithm (routine LMDIF of the MINPACK software suite [53]) to refine the optimal parameter values. The procedure constrains the FRP at a value of 24 hours and the goodness of fit includes both RMS error and a penalty proportionnal to the Eulerian distance between current parameter set and the reference one obtained in [40]. This penalty maximizes correlation between the different best-fitting parameter sets and makes their comparison easier. Numerical integration of ordinary differential equations was performed with the SEULEX algorithm [54]. The exhaustivity of the harmony search stage and the convergence of the adjustment were monitored by checking that the optimum was reached repeatedly.

4.5 Probability of adjustment by free-running oscillators

In order to show that the simultaneous adjustment of photoperiodic data by free-running oscillators is biologically significant, it is important to show that such a numerical result cannot be obtained by chance. We therefore generated a large number of random target profiles which were then fed to the optimization procedure. The random protein profiles (one for TOC1 and one for CCA1) featured a single peak per period, obtained by interpolating three control points with a cubic spline. A TOC1–CCA1 delay was then chosen at random between 2 and 12 hours. This yields smoothly varying profiles similar to the experimental ones and to those which can be generated by a free-running 4-ODE model.

We found that for this set of random profiles, the probability of obtaining a RMS error as good as obtained in Fig. 4 is always lower than 0.4. The probability of obtaining 11 such adjustments is thus bounded above by $4 \cdot 10^{-5}$.

Acknowledgments

This work has been supported by Ministry of Higher Education and Research, Nord-Pas de Calais Regional Council and FEDER through the Contrat de Projets État-Région (CPER) 2007 2013.

References

- [1] Alon, U. (2006) *An introduction to systems biology: design principles of biological circuits*, Chapman Hall/CRC, New York.
- [2] Savageau, M. (2001) Design principles for elementary gene circuits: Elements, methods, and examples, *Chaos* **11**, 142–159.

- [3] Novak, B. & Tyson, J. (2008) Design principles of biochemical oscillators, *Nat. Rev. Mol. Cell Biol.* **9**, 981–991.
- [4] Hartwell, L., Hopfield, J., Leibler, S. & Murray, A. (1999) From molecular to modular cell biology, *Nature* **402**, C47–C52.
- [5] Mengel, B., Hunziker, A., Pedersen, L., Trusina, A., Jensen, M. H. & Krishna, S. (2010) Modeling oscillatory control in NF- κ B, p53 and wnt signaling, *Curr. Opin. Genet. Dev.* **20**, 656–664.
- [6] Kobayashi, T. & Kageyama, R. (2009) Dynamic advances in NF-KB signaling analysis, *Sci Signal* **2**, 47.
- [7] Alon, U. (2003) Biological networks: The tinkerer as an engineer, *Science* **301**, 1866–1867.
- [8] Rand, D. A., Shulgin, B. V., Salazar, D. & Millar, A. J. (2004) Design principles underlying circadian clocks, *J. Roy. Soc. Interface* **1**, 119–130.
- [9] Rand, D. (2008) Mapping global sensitivity of cellular network dynamics: sensitivity heat maps and a global summation law, *J. Roy. Soc. Interface* **5**, S59–S69.
- [10] Stelling, J., Sauer, U., Szallasi, Z., Doyle, F. & Doyle, J. (2004) Robustness of cellular functions, *Cell* **118**, 675–685.
- [11] Kollmann, M., Lovdok, L., Bartholome, K., Timmer, J. & Sourjik, V. (2005) Design principles of a bacterial signalling network, *Nature* **438**, 504–507.
- [12] Ukai, H. & Ueda, H. R. (2010) Systems biology of mammalian circadian clocks, *Annu. Rev. Physiol.* **72**, 579–603.
- [13] Yamada, Y. R. & Forger, D. B. (2010) Multiscale complexity in the mammalian circadian clock, *Curr. Opin. Genet. Dev.* **20**, 626–633.
- [14] Roenneberg, T., Chua, E. J., Bernardo, R. & Mendoza, E. (2008) Modelling biological rhythms, *Curr. Biol.* **18**, R826–R835.
- [15] Dunlap, J. C. (1999) Molecular bases for circadian clocks, *Cell* **96**, 271–290.
- [16] Young, M. W. & Kay, S. (2001) Time zones: a comparative genetics of circadian clocks, *Nature Genetics* **2**, 702–715.
- [17] Imaizumi, T. & Kay, S. A. (2006) Photoperiodic control of flowering: not only by coincidence, *Trends Plant Sci.* **11**, 550–558.
- [18] Geier, F., Becker-Weimann, S., Kramer, A. & Herzel, H. (2005) Entrainment in a Model of the Mammalian Circadian Oscillator, *J. Biol. Rhythms* **20**, 83–93.

- [19] Salazar, J. D., Saithong, T., Brown, P. E., Foreman, J., Locke, J. C. W., Halliday, K. J., Carre, I. A., Rand, D. A. & Millar, A. J. (2009) Prediction of photoperiodic regulators from quantitative gene circuit models, *Cell* **139**, 1170–1179.
- [20] Edwards, K. D., Akman, O. E., Knox, K., Lumsden, P. J., Thomson, A. W., Brown, P. E., Pokhilko, A., Kozma-Bognar, L., Nagy, F., Rand, D. A. & Millar, A. J. (2010) Quantitative analysis of regulatory flexibility under changing environmental conditions, *Mol. Syst. Biol.* **6**, 424.
- [21] Johnson, C., Elliott, J. & Foster, R. (2003) Entrainment of circadian programs, *Chronobiol. Int.* **20**, 741–774.
- [22] Bagheri, N., Taylor, S. R., Meeker, K., Petzold, L. R. & Doyle, F. J. (2008) Synchrony and entrainment properties of robust circadian oscillators, *J. Roy. Soc. Interface* **5**, S17–S28.
- [23] Mondragon-Palomino, O., Danino, T., Selimkhanov, J., Tsimring, L. & Hasty, J. (2011) Entrainment of a Population of Synthetic Genetic Oscillators, *Science* **333**, 1315–1319.
- [24] Abraham, U., Granada, A. E., Westermarck, P. O., Heine, M., Kramer, A. & Herzog, H. (2010) Coupling governs entrainment range of circadian clocks, *Mol. Syst. Biol.* **6**, 438.
- [25] Barkai, N. & Leibler, S. (2000) Biological rhythms: Circadian clocks limited by noise, *Nature* **403**, 267–268.
- [26] Gonze, D., Halloy, J. & Goldbeter, A. (2002) Robustness of circadian rhythms with respect to molecular noise, *Proc. Nat. Acad. Sci. USA* **99**, 673–678.
- [27] Zwicker, D., Lubensky, D. K. & ten Wolde, P. R. (2010) Robust circadian clocks from coupled protein-modification and transcription-translation cycles, *Proc. Natl. Acad. Sci. USA* **107**, 22540–22545.
- [28] Pittendrigh, C. S. (1954) On temperature independence in the clock system controlling emergence time in drosophila, *Proc. Natl. Acad. Sci. USA* **40**, 1018–1029.
- [29] Rensing, L. & Ruoff, P. (2002) Temperature effect on entrainment, phase shifting, and amplitude of circadian clocks and its molecular bases, *Chronobiol. Int.* **19**, 807–864.
- [30] Beersma, D. G. M., Daan, S. & Hut, R. A. (1999) Accuracy of circadian entrainment under fluctuating light conditions: Contributions of phase and period responses, *J. Biol. Rhythms* **14**, 320–329.

- [31] Troein, C., Locke, J. C. W., Turner, M. S. & Millar, A. J. (2009) Weather and seasons together demand complex biological clocks, *Current Biology* **19**, 1961–1964.
- [32] Taylor, S. R., Webb, A. B., Smith, K. S., Petzold, L. R. & Doyle, F. J. (2010) Velocity response curves support the role of continuous entrainment in circadian clocks, *J. Biol. Rhythms* **25**, 138–149.
- [33] Courties, C., Vaquer, A., Troussellier, M., Lautier, J., Chretiennot-Dinet, M. J., Neveux, J., Machado, M. C. & Claustre, H. (1994) Smallest eukaryotic organism, *Nature* **370**, 255.
- [34] Chretiennot-Dinet, M. J., Courties, C., Vaquer, A., Neveux, J., Claustre, H., Lautier, J. & Machado, M. C. (1995) A new marine picoeukaryote : *Ostreococcus tauri* gen. et sp. nov. (chlorophyta, prasinophyceae), *Phycologia* **4**, 285–292.
- [35] Derelle, E., Ferraz, C., Rombauts, S., Rouzé, P., Worden, A. Z., Robbens, S., Partensky, F., Degroeve, S., Echeynié, S., Cooke, R., Saeys, Y., Wuyts, J., Jabbari, K., Bowler, C., Panaud, O., Piégu, B., Ball, S. G., Ral, J.-P., Bouget, F.-Y., Piganeau, G., De Baets, B., Picard, A., Delseny, M., Demaille, J., de Peer, Y. V. & Moreau, H. (2006) Genome analysis of the smallest free-living eukaryote *Ostreococcus tauri* unveils many unique features, *Proceedings of the National Academy of Sciences* **103**, 11647–11652.
- [36] Moulager, M., Monnier, A., Jesson, B., Bouvet, R., Mosser, J., Schwartz, C., Garnier, L., Corellou, F. & Bouget, F.-Y. (2007) Light-dependent regulation of cell division in *ostreococcus*: evidence for a major transcriptional input, *Plant Physiol.* **144**, 1360–1369.
- [37] Monnier, A., Liverani, S., Bouvet, R., Jesson, B., Smith, J. Q., Mosser, J., Corellou, F. & Bouget, F.-Y. (2010) Orchestrated transcription of biological processes in the marine picoeukaryote *Ostreococcus* exposed to light/dark cycles, *BMC Genomics* **11**, 192.
- [38] Corellou, F., Schwartz, C., Motta, J.-P., Djouani-Tahri, E. B., Sanchez, F. & Bouget, F.-Y. (2009) Clocks in the green lineage: comparative functional analysis of the circadian architecture in the picoeukaryote *ostreococcus*, *Plant Cell* **21**, 3436–3449.
- [39] Thommen, Q., Pfeuty, B., Morant, P., Corellou, F., Bouget, F. & Lefranc, M. (2010) Robustness of circadian clock to daylight fluctuations: hints from the picoeukaryote *ostreococcus tauri*., *Plos Comput. Biol.* **6**, e1000990. doi:10.1371/journal.pcbi.1000990.

- [40] Morant, P.-E., Thommen, Q., Pfeuty, B., Vandermoere, C., Corellou, F., Bouget, F.-Y. & Lefranc, M. (2010) A robust two-gene oscillator at the core of *Ostreococcus tauri* circadian clock, *Chaos* **20**, 045108.
- [41] Troein, C., Corellou, F., Dixon, L. E., van Ooijen, G., O'Neill, J. S., Bouget, F.-Y. & Millar, A. J. (2011) Multiple light inputs to a simple clock circuit allow complex biological rhythms, *Plant J.* **66**, 375–385.
- [42] Moulager, M., Corellou, F., Verge, V., Escande, M.-L. & Bouget, F.-Y. (2010) Integration of light signals by the retinoblastoma pathway in the control of S phase entry in the picophytoplanktonic cell *Ostreococcus*, *PLoS Genet.* **6**, e1000957.
- [43] Gutenkunst, R. N., Waterfall, J. J., Casey, F. P., Brown, K. S., Myers, C. R. & Sethna, J. P. (2007) Universally sloppy parameter sensitivities in systems biology models, *PLoS Comput. Biol.* **3**, e189.
- [44] Pfeuty, B., Thommen, Q. & Lefranc, M. (2011) Robust entrainment of circadian oscillators requires specific phase response curves, *Biophys J* **100**, 2557–2565.
- [45] Akman, O. E., Guerriero, M. L., Loewe, L. & Troein, C. (2010) Complementary approaches to understanding the plant circadian clock, in Merelli, E. & Quaglia, P., eds., *Proceedings Third Workshop From Biology To Concurrency and back*, Paphos, Cyprus, 27th March 2010, volume 19 of *Electronic Proceedings in Theoretical Computer Science*, 1–19, Open Publishing Association.
- [46] Djouani-Tahri, E., Motta, J.-P., Bouget, F.-Y. & Corellou, F. (2010) Insights into the regulation of the core clock component *toc1* in the green picoeukaryote *ostreococcus*., *Plant Signal Behav.* **5**, 332–335.
- [47] Djouani-Tahri, E.-B., Christie, J. M., Sanchez-Ferandin, S., Sanchez, F., Bouget, F.-Y. & Corellou, F. (2011) A eukaryotic LOV-histidine kinase with circadian clock function in the picoalga *ostreococcus*, *Plant J.* **65**, 578–588.
- [48] Comas, M., Beersma, D. G. M., Spoelstra, K. & Daan, S. (2006) Phase and period responses of the circadian system of mice (*Mus musculus*) to light stimuli of different duration, *J. Biol. Rhythms* **21**, 362–372.
- [49] Tsumoto, K., Kurosawa, G., Yoshinaga, T. & Aihara, K. (2011) Modeling light adaptation in circadian clock: Prediction of the response that stabilizes entrainment, *PLoS ONE* **6**, e20880.
- [50] Rand, D. A., Shulgin, B. V., Salazar, J. D. & Millar, A. J. (2006) Uncovering the design principles of circadian clocks: mathematical analysis of flexibility and evolutionary goals, *J. Theor. Biol.* **238**, 616–635.

- [51] Comas, M., Beersma, D., Hut, R. & Daan, S. (2008) Circadian phase resetting in response to light-dark and dark-light transitions, *J. Biol. Rhythms* **23**, 425–434.
- [52] Geem, Z. W., Kim, J. H. & Loganathan, G. V. (2001) A new meta-heuristic algorithm for continuous engineering optimization: harmony search theory and practice, *SIMULATION* **76**, 60.
- [53] Moré, J., Garbow, B. & Hillstom, K. (1999), MINPACK, version 1, Available: <http://www.netlib.org/minpack/>. Accessed 15 January 2009.
- [54] Hairer, E. & Wanner, G. (1996) *Solving Ordinary Differential Equations II. Stiff and Differential-Algebraic Problems.*, volume 14 of *Springer Series in Comput. Mathematics*, Springer-Verlag.